A. Nikolaeva[1,2], L. Konopko[1,2], T. Huber[3], P. Bodiul[1,4], I. Popov[1], E. Moloshnik[1], I. Gergishan[1]

[1]D.Gitsu Institute of Electronic Engineering and Nanotechnologies
of the Academy of Sciences of Moldova, Academiei str., 3/3,
Kishinev, MD-2028, Republic of Moldova;
[2]International Laboratory of High Magnetic Fields and Low Temperatures,
ul. Gajowicka 95, Wroclaw, 53-421, Poland;
[3]Howard University, 500 College St. NW, Washington, USA
[4]Technical University of Moldova, 168, Stefan cel Mare blvd., Kishinev,
MD-2004, Republic of Moldova

THE IMPACT OF DIMENSIONS, MAGNETIC FIELD, ELASTIC DEFORMATION ON THE THERMOELECTRIC FIGURE OF MERIT OF THE TOPOLOGICAL INSULATOR WIRES BASED ON SEMICONDUCTOR $Bi_{1-x}Sb_x$ WIRES

This paper presents the experimental results of a study of thermoelectric properties of the topological insulator (TI) wires based on semiconductor $Bi_{1-x}Sb_x$ wires. Glass-coated semiconductor Bi-17 at % Sb wires prepared by the Ulitovsky liquid phase casting method were single crystals strictly of cylindrical shape with diameters ranging from 100 nm to 1000 nm and crystallographic orientation (1011) along the wire axis. It has been found that the energy gap ΔE_g in the Bi-17 at % Sb wires increases with decreasing wire diameter as 1/d, which is a manifestation of the quantum size effect. At low temperatures, a deviation from the exponential temperature dependence of the resistance $R \sim \exp(E/2k_BT)$ is observed; the conductivity of the wires increases with decreasing diameter which is most pronounced at T = 4.2 K due to the TI properties, in particular, the presence of surface states with high conductivity. The effect of temperature, magnetic field, elastic deformation, and the diameter of the Bi-17 at % Sb wires on power factor P.f. = $\alpha^2\sigma$ in the temperature range of 4.2 – 300 K has been studied. It has been shown that the maximum P.f. value is achieved at T = 300 K for wires with d = 100 nm and P.f. decreases with increasing diameter d. It has been found that both the magnetic field (H // I) and the elastic deformation of the wires lead to increase in the power factor by 35 – 40 % at T > 150 K; this finding opens up the possibility of optimizing the thermoelectric parameters of $Bi_{1-x}Sb_x$ TI based wires for use in thermoelectric energy converters.

Key words: thermoelectricity, semiconductor nanowires, topological insulator, quantum size effect, deformation.

Introduction

It is known that $Bi_{1-x}Sb_x$ alloys in the semiconductor concentration range for many years have been the best magnetothermoelectric material in the intrinsic region and have been widely used as *n*-legs in thermoelectric power converters at low temperatures ($40 < T < 150$ K) [1 – 6]. $Bi_{1-x}Sb_x$ ($0 \le x \le 1$) alloys form a continuous series of solid solutions. With a change in *Sb* concentration from 0 to 1, the energy spectrum of *Bi* is being constantly rearranged into *Sb* spectrum, forming in the concentration range ($0.08 < x < 0.25$) a semiconductor phase with maximum gap 25 meV (Fig. 1) [7].

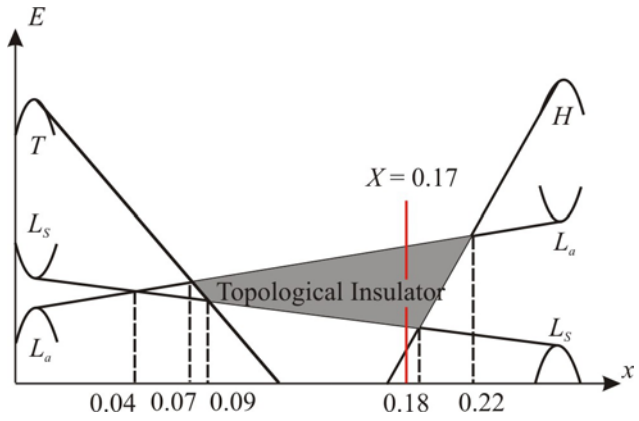

Fig. 1. Schematic of energy spectrum rearrangement in $Bi_{1-x}Sb_x$ alloys versus the concentration of Sb (0 < x < 0.25 Sb).

Optimization of thermoelectric materials includes three parameters - thermopower α (the Seebeck coefficient), electric conductivity of material σ and thermal conductivity $\chi = (\chi_e + \chi_p)$, where χ_e is electron thermal conductivity and χ_p is lattice thermal conductivity. The thermoelectric figure of merit $Z = \alpha^2\sigma/\chi_e + \chi_p$ [2].

Long-term manipulation of these parameters has not resulted in the improvement of thermoelectric figure of merit ($Z > 1$), the reasons for which have been considered in detail in papers and reviews [3 – 9].

A new impetus to development of thermoelectric materials was given by theoretical works of M.S. Dresselhaus with co-authors [10 – 13] dedicated to low-dimensional quantum systems (wires, films, quantum dots) based on *Bi* and $Bi_{1-x}Sb_x$ materials in which quantum size effects are most pronounced and in which considerable improvement of thermoelectric figure of merit *ZT* was predicted. It was shown that sample dimensions (thickness or diameter *d*) become an additional parameter affecting the thermoelectric figure of merit of material, when at least one of sample dimensions *d* is commensurate to the Broglie wavelength $\lambda = \frac{h}{p}$.

The reason for this is increase in the density of states of charge carriers $g(E)$ leading in quantum systems to increase of thermopower α, as well as decrease in thermal conductivity χ due to reduction of the mean free path of carriers and phonons because of additional scattering on the boundaries. Rapid development of nanotechnologies promoted experimental development of thermoelectric nanomaterials. However, experimental results obtained during recent 15 – 20 years are more modest than theoretical. Several papers [14, 15] reported on obtaining $ZT = 2$ at $T = 300$ K in Bi_2Te_3/Sb_2Te_3 superlattices and $ZT = 3$ at $T = 450$ K in quantum dot *PbTe/PbSeTe* superlattices. The thermoelectric achievements in low-dimensional semiconductors are most fully covered in the paper by J.P. Heremans [16]. A particularly complex issue is reproducibility of results and their real use in thermoelectricity.

In recent years much attention has been given to a new class of materials – topological insulators [17 – 19] which include $Bi_{1-x}Sb_x$ alloys in semiconductor region (Fig. 1). In [20] it was shown that the state of topological insulator is realized in semiconductors with inverted spectrum.

It was long believed that in the semimetal $Bi_{1-x}Sb_x$ alloys with $x < 0.04$ the energy spectrum at point *L* is inverted and in the alloys with $x > 0.04$ it is direct, since in the electron and hole spectrum at point *L* the ”saddle point” was not found. However, in 1998 the authors of [21] discovered the “saddle point” in the electron and hole spectra at point *L* of the Brillouin zone, at $x \approx 0.15$, so with increase in *k*,

the $E(k)$ relationship acquires a double-humped shape. Thus, the spectrum of *Bi* at point *L* is direct, and the spectrum of $Bi_{1-x}Sb_x$ ($0.04 < x < 1$) alloys is inverted, and so in these alloys in semiconductor region one should expect manifestation of TI properties, particularly in low-dimensional systems. Semiconductor $Bi_{1-x}Sb_x$ alloys were the first open thee-dimensional TI with five intersected Fermi levels of surface band [22, 23]. Studies by means of angle-resolved photoemission spectroscopy (ARPES) have proved the existence of surface states in the semiconductor $Bi_{1-x}Sb_x$ alloys with the dispersion law which enables one to refer these alloys to the class of topological insulators [24].

High carrier mobilities from the surface states were found in $Bi_{0.9}Sb_{0.1}$ TI [25]. Thermoelectric figure of merit improvement in topological insulators was predicted in [14, 19, 26].

To understand macroscopic properties of TI surface state and study the opportunities of their practical use, it is necessary to perform transport studies. The purpose of the present paper was to study manifestation of TI properties and to investigate the thermoelectric properties of *Bi*-17 at % *Sb* TI wires depending on diameter, temperature, magnetic field and elastic deformation.

Samples and experimental procedure

Thin single crystal wires were prepared by the Ulitovsky liquid phase casting method [27, 28]. Single crystal *Bi*-17 at % *Sb* ingot, prepared by zone recrystallization method, was used as the initial material.

Crystallization of microwire core of bismuth and $Bi_{1-x}Sb_x$ alloys proceeds with strong overcooling of melt at the crystallization front. For bismuth, ultimate overcooling depth occurs at casting rate 10 m/s and reaches 40 – 50 °C. Strong overcooling and high crystallization rates contribute to growth of single crystal core and retention of stoichiometric composition of *Bi*-17 at % *Sb* alloy.

Wire diameter was measured by optical microscope Biolam with magnification 1350. Test diameter measurements were made on scanning electron microscope (SEM) Vega Tescan 5130 MM.

Monocrystallicity of *Bi*-17 at % *Sb* wires and their crystallographic orientation was established by means of rotation X-ray diagrams. Samples of all diameters had orientation (1011) along the wire axis. In so doing, like in the wires of pure *Bi* [29], the trigonal C_3 axis is inclined to the wire axis at an angle of ~ 20º, and the C_3 axis is normal to that axis.

Glass-coated wires were arranged on a plate of copper-clad paper-based laminate with the cut-out copper contact stripes onto which *InGa* eutectics was deposited which at 300 K was in liquid state. A contact was created due to wetting of *InGa* wire ends with eutectics, to provide contact ohmicity. The length of the sample was 1 ÷ 3 mm. The plate with the wire was placed into a special holder which was immersed into cryostat for low-temperature measurements. A differential thermocouple *Cu*-*Cu*(0.05 *Fe*) having thermal contact with the cold and heated wire ends was used for measuring temperature difference on sample ends. Temperature gradient was created from 0.5 K to 2 K depending on the measurement temperature.

The resistance was measured by two-contact method with the error not more than 1 %, and total error of thermopower measurement was ~ 10 %.

The arrangement of principal crystallographic axes and monocrystallicity of the wires of all diameters have been confirmed by investigation of angle rotation diagrams of transverse magnetoresistance $R(\theta)$ ($H \perp I$) in various magnetic fields (0.5 ÷ 14 T) at T = 300 K, 150 K, 80 K, 4.2 K.

Example of recording angle rotation diagrams $\Delta R/R(\theta)$ of *Bi*-17 at % *Sb* wire with d = 200 nm at 150 K and different values of magnetic field H is represented in Fig. 2.

Angular dependences of transverse magnetoresistance are symmetrical with respect to direction $\theta = 0$ and $\theta = 90^0$, which fully corresponds to phenomenological expressions [30]. It should be noted that unlike rotation diagrams of transverse magnetoresistance, on the wires and single crystals of *Bi* and semi-metal $Bi_{1-x}Sb_x$ alloys in high magnetic fields minimum is formed at $H \parallel C_3$, and maximum – at $H \parallel C_2$.

This data is in good agreement with the results of [24] obtained on the bulk single crystals of corresponding composition and orientation.

Deformation dependences of resistance $R(\xi)$ and thermopower $\alpha(\xi)$, where $\xi = l - l_0/l_0$, l_0 is sample length without tensile load were measured to 1.5 – 2 % of relative elongation, as described in [31, 32]. Particular attention was focused on deformation elasticity condition which was estimated by the reproducibility of results at numerous stretching cycles for each temperature.

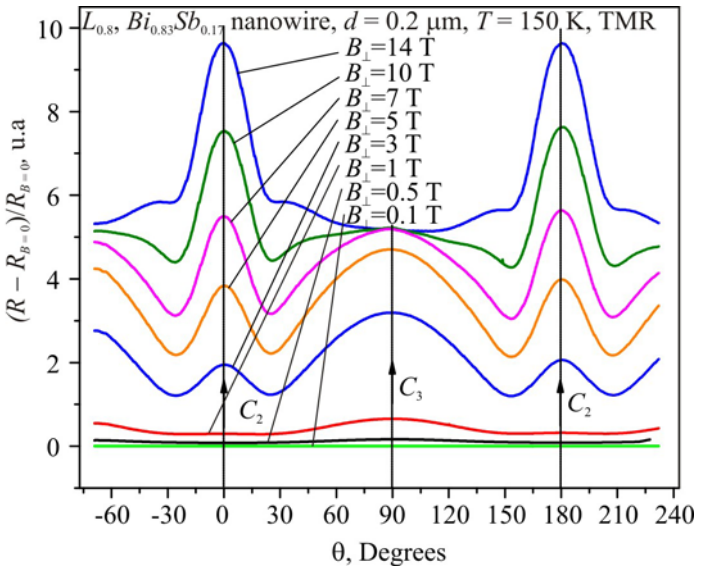

Fig. 2. Transverse magnetoresistance rotation diagrams of Bi-17 at % Sb wire, T = 150 K, d = 200 nm, for different magnetic field values.

Measurements in a magnetic field were performed in a longitudinal configuration $H \parallel I$, $H \parallel \Delta T$) in the region of magnetic fields up to 14 T in the Bitter-magnet field at temperatures 2 – 300 K in the International Laboratory of High Magnetic Fields and Low Temperatures (Wroclaw, Poland).

Discussion of the results

Fig. 3 shows temperature dependences of relative resistance $\Delta R/R(T)$, where $\Delta R = R_T - R_{300}$, for semiconductor *Bi*-17 at % *Sb* wires of different diameters, in the temperature range of 1.5 – 300 K. At 300 K relative resistance ρ is practically independent of wire diameter *d*. With decrease in temperature, resistance grows for the wires of all diameters under study, and exponential areas, $R \sim \exp(\Delta E/2k_BT)$, appear on the $R(T)$ dependences.

The slope of exponential areas and the area of their existence depend on the wire diameter *d*. With decreasing wire diameter *d*, the area of linear dependence $\rho(10^3/T)$ is displaced toward higher temperatures (Fig. 3, inset). From the linear dependences $\rho(10^3/T)$ it follows that thermal gap essentially depends on the wire diameter *d*, increasing from the value 20 – 22 meV, for the wire with d = 1100 nm, typical for the bulk samples of similar composition, to the value ΔE = 42 meV for the wire with d = 100 nm.

Such dependence on the wire diameter d is a manifestation of quantum size effect leading to semimetal-semiconductor transition in semimetal wires of pure Bi and $Bi_{1-x}Sb_x$ ($x < 0.04$), and in semiconductor $Bi_{1-x}Sb_x$ wires [33, 34] – to gap increase with decreasing wire diameter d [12, 27, 28, 33, 34].

It should be noted that in $Bi_{1-x}Sb_x$ alloys c $0.15 < x < 0.22$ the thermal gap found from the experimental dependences of resistivity on temperature, is indirect gap ΔE_{LH}, equal to the distance between the bottom of conduction band and the ceiling of valence band in H (Fig. 1). However, in the general case from the $\rho(T)$ dependences of semiconductor $Bi_{1-x}Sb_x$ alloys the "effective" thermal gap ΔE_T is determined which is observed as a result of thermal generation of carriers both through ΔEg_L gap and through ΔE_{LT} or ΔE_{LH}. According to Fig. 3 (inset below) the energy gap exponentially grows with decreasing diameter $\Delta E \sim \exp(d)$.

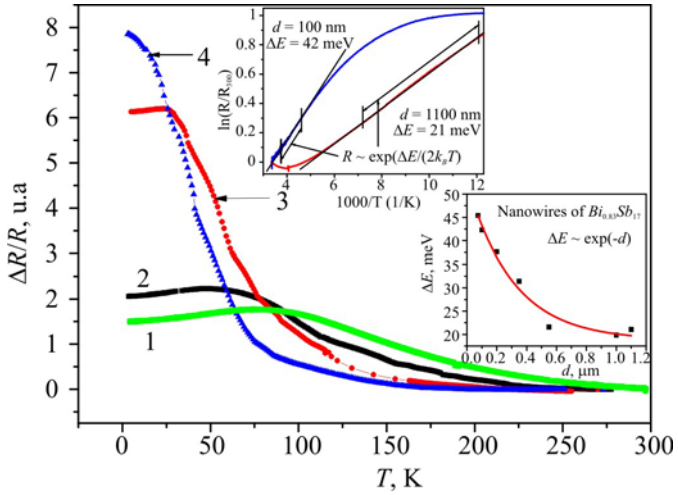

Fig. 3. Temperature dependences of reduced resistance ΔR/R(T) in the Bi-17 % Sb wires of different diameters: 1. d = 100 nm, 2. d = 200 nm, 3. d = 600 nm, 4. d = 900 nm. On the inset above: $R(10^3/T)$ dependences for the wires with d = 200 nm and d = 1100 nm; below - dependences of ΔEg gap on the wire diameter d.

In low-temperature region $T < 100$ K there is major change in the temperature dependences $R(T)$ (Fig. 3) with decreasing wire diameter d. There was a deviation from the exponential growth of $R(T)$ with decrease in temperature and plateau formation at $T \to 4.2$ K. The temperature whereby this deviation occurs is displaced toward higher temperatures with decreasing wire diameter d. In fact, at 4.2 K there is an increase in the conductivity of semiconductor Bi-17 at % Sb wires by a factor of ≈ 5, with increasing diameter from 1000 nm to 100 nm (Fig. 3).

Such $R(T)$ behaviour in low-temperature region can be explained from the standpoint of manifestation of TI properties, namely the emergence of high-conductivity surface states the contribution of which increases with decreasing wire diameter and the resistance drops. In TI, conductive surface properties result from strong spin-orbit interaction which leads to the emergence of spin-split topological surface states with the Dirac type of dispersion, i.e. linear dependence of energy on pulse [35].

There were also investigated temperature dependences of thermopower $\alpha(T)$ in the temperature range of 4.2 – 300 K for the wires of different diameters (Fig. 4).

For the wires of all investigated diameters the thermopower is negative in the entire temperature range. With decreasing temperature, the thermopower increases in the absolute value

reaching -150 μV/K in the region of 30 – 50 K. With decrease in temperature to 4.2 K, the thermopower decreased to -20 μV/K for the wires of all investigated diameters.

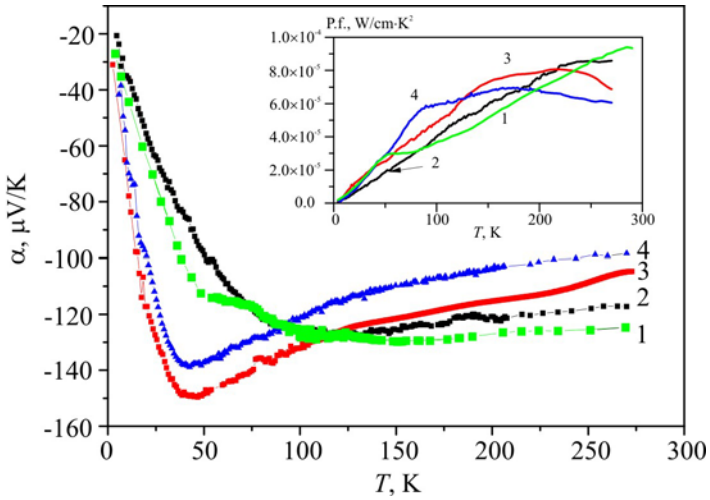

Fig. 4. Temperature dependences of thermopower α(T) of $Bi_{1-x}Sb_x$ wires of different diameters: 1. d = 100 nm, 2. d = 200 nm, 3. d = 600 nm, 4. d = 900 nm. In the inset: temperature dependences of power factor P.f. = $\alpha^2\sigma(T)$.

With decreasing wire diameter, maximum thermopower value is reduced and the peak is displaced toward higher temperatures. Thermopower decrease in the thin wires of semiconductor $Bi_{1-x}Sb_x$ alloys is due to the effect of surface scattering on the mean free path of electrons determining at $T < 100$ K the sign and value of thermopower. The drop in the effective mean free path of electrons with decreasing wire diameter results in the reduction of their contribution to thermopower, which is the consequence of classical size effect manifestation.

Dependences of power parameter P.f. = $\alpha^2\sigma$ on the temperature and wire diameter d were determined according to thermopower $\alpha(T)$ and resistance $R(T)$ data and represented in the inset of Fig. 4. Maximum value P.f. = 8 10^{-5} W/cm K^2 is achieved at 300 K in the wires with the minimum diameter d = 100 nm (Fig. 4, curve 1).

The effect of magnetic field $H \parallel I$, $\|\Delta T$ and elastic tensile deformation on the thermoelectric figure of merit of the *Bi*-17 at % *Sb* wires was investigated at different temperatures.

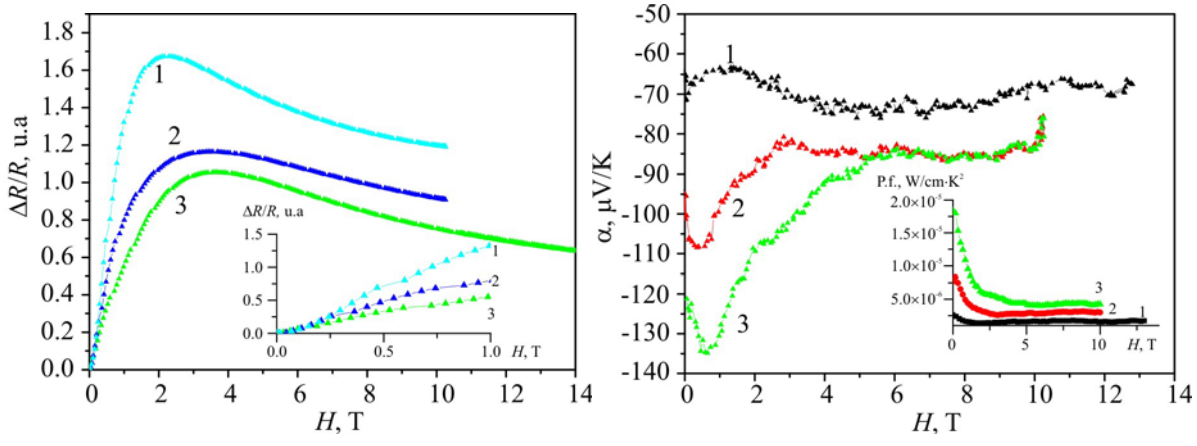

a) *b*)

Fig. 5. Field dependences of relative resistance ΔR/R(H) (a) and thermopower α(H) (b) of Bi – 17% Sb wire, d = 200 nm at different temperatures: 1. T = 17 K, 2. T = 38 K, 3. T = 64 K. In the inset (a) initial sections (up to 1 T) of the field dependences of ΔR/R(H). In the inset (b): field dependence of power factor P.f.(H), at different temperatures: 1. T = 17 K, 2. T = 38 K, 3. T = 64 K.

Fig. 5 and 6 represent the magnetic field dependences of resistance (*a*) $\Delta R/R(H)$ ($H \parallel I$) and thermopower (*b*) $\alpha(H)$ ($H \parallel \Delta T$) at fixed temperature values of the *Bi*-17 at % *Sb* wires, $d = 200$ nm (Fig. 5) and $d = 100$ nm (Fig. 6).

With increasing magnetic field, the resistance grows at all temperatures, however, in weak magnetic fields with a rise in temperature resistance growth is decelerated (insets in Fig. 5*a* and Fig. 6*a*), whereas increase in thermopower $\alpha(H)$ is enhanced (Fig. 5*b*, 6*b*).

In the *Bi*-17 at % *Sb* wires with $d = 200$ nm resistance growth versus magnetic field ($H = 2$ T) is 80 % at $T = 64$ K, and in the wires with $d = 100$ nm resistance increases by 18 % at $T = 52$ K. Weak thermopower increase in magnetic fields up to 2 *T* leads to reduction of power factor in the wires with $d = 200$ nm (curve 3 in the inset of Fig. 5*b*) and stabilization of P.f. for the wires with $d = 100$ nm (curve 2 Fig. 7*a*).

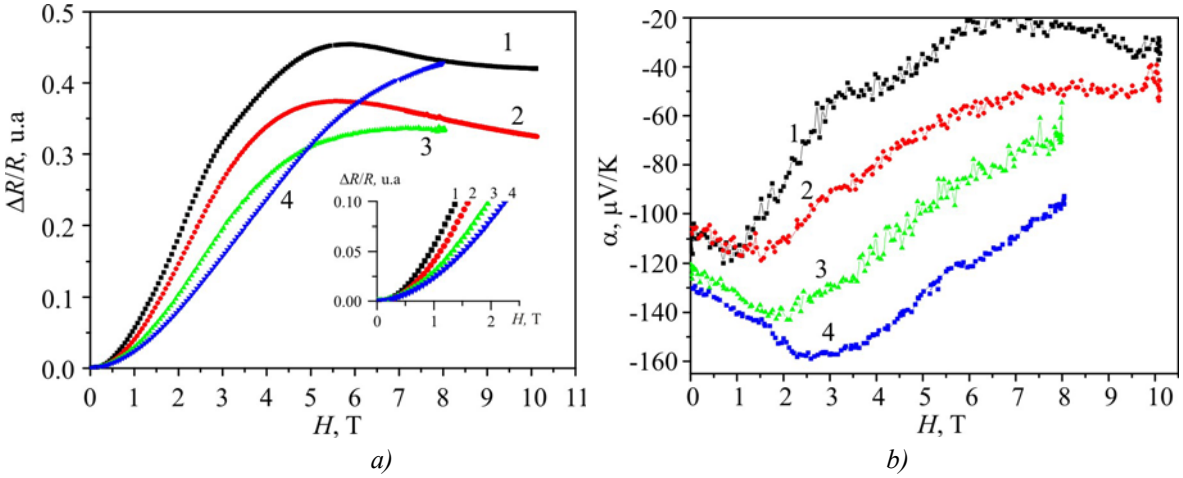

Fig. 6. Field dependences of relative resistance ΔR/R(H) (a) and thermopower α(H) (b) of the Bi-17 at % Sb wire, d = 100 nm, at different temperatures: 1. T = 7 K, 2. T = 52 K, 3. T = 100 K, 4. T = 145 K. In the inset (a) the initial sections of the field dependences of ΔR/R(H).

At higher temperatures the situation is different. As is seen from Fig. 6*b*, at $T = 143$ K for the wires with $d = 100$ nm, the thermopower increases in magnetic fields 2.5 *T* by ~ 20 % (curve 4), whereas the resistance increases by ~ 10 % under the same conditions. The calculated value of power factor P.f. = $\alpha^2\sigma$ versus a magnetic field points to P.f. increase by ~ 40 % in a magnetic field 2.5 *T* (Fig. 7*a*, curve 4).

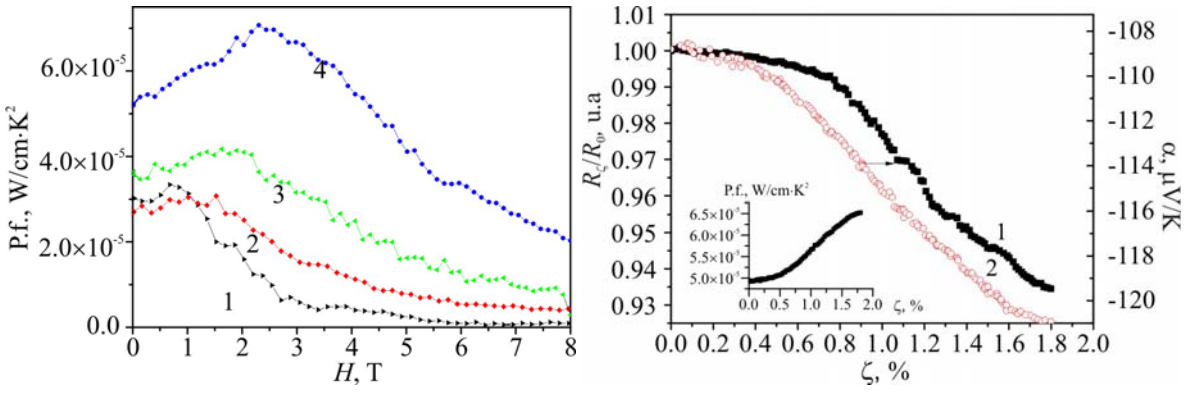

Fig. 7. (a) Field dependences of power factor P.f. of the Bi-17 at % Sb wire, d = 100 nm, at different temperatures: 1. T = 7 K, 2. T = 52 K, 3. T = 100 K, 4. T = 145 K. (b) Deformation dependences of relative resistance $R_\xi/R_0(H)$ - curve 1, and thermopower $\alpha(\xi)$ - curve 2, the Bi-17 at % Sb wires, d = 100 nm at T = 146 K. Inset: deformation dependence of power factor P.f. (ξ).

There were also investigated deformation dependences (tensile deformation) of resistance $R(\xi)$ and thermopower $\alpha(\xi)$ at different temperatures. Fig. 7*b* shows deformation dependences of resistance $R_\xi/R_0(H)$ -1 and thermopower $\alpha(\xi)$ – 2 at $T = 146$ K, ($\xi = l\text{-}l_0/l_0$, where l_0 is wire tension length).

As can be seen from Fig. 7*b*, elastic tensile deformation of thin wires ($d = 100$ nm) to 1.8 % of relative elongation leads to resistance decrease and increase of thermopower absolute value, which results in P.f. increase by ~ 30 % at 146 K.

Thus, magnetic field and elastic deformation lead to an increase in thermoelectric figure of merit of the semiconductor *Bi*-17 % *Sb* wires with $d = 100$ nm, which opens up the possibility of purposeful control over thermoelectric parameters of nanowires based on the semiconductor $Bi_{1-x}Sb_x$ alloys. It is interesting to study the thermoelectric figure of merit with a simultaneous impact of a weak magnetic field and deformation in high-temperature region 200 – 300 K.

Conclusions

Studies of magnetothermoelectric properties of single-crystal *Bi*-17 at % *Sb* TI wires with diameters from 100 nm to 1000 nm have shown that, on the one hand, manifestation of quantum size effect leads to increase in the energy gap *Eg* with decreasing wire diameter: $\Delta Eg \sim 1/d$, and, on the other hand, manifestation of TI properties in low-temperature region (4.2 K) leads to increase in conductivity σ with decreasing wire diameter due to formation of high-conductivity surface states of TI.

It was established that both a weak magnetic field and elastic tensile deformation lead to power factor increase by $\approx$ 30 – 40 % in the wires with a minimum diameter 100 nm at temperatures $\geq$ 140 K.

Decreasing diameter d of the wires and study of their thermoelectric parameters at $T > 150$ K with a simultaneous impact of deformation and magnetic field will enable one to optimize magnetothermoelectric parameters of $Bi_{1-x}Sb_x$ wires for their use in thermoelectric power converters.

This work was performed with support of STCU grant # 5986.

References

1. A.F. Ioffe, *Physics of Semiconductors* (Academic Press Inc, New York, 1960), 178 – 179p.
2. H.J. Goldsmid, *Applications of Thermoelectricity* (London: Methuen & Co. Ltd., 1960).
3. W.M. Yim, A. Amith, Alloys for Magneto-Thermoelectric and Thermomagnetic Cooling. *Solid-State Electronics* **15**(10), 1141 – 1165 (1972).
4. G.A. Ivanov, V.A. Kulikova, V.L. Naletov, A.F. Panarin, and A.R. Regel, Thermoelectric Figure of Merit of Pure and Doped Bismuth-Antimony Alloys in a Magnetic Field, *Semiconductors* **6**(7), 1296 – 1299 (1972).
5. L.I. Anatychuk, *Thermoelements and Thermoelectric Devices: Reference Book* (Kyiv: Naukova Dumka, 1979), 768 p.
6. N.A. Rodionov, G.A. Ivanov, and N.A. Redko, Thermoelectric Figure of Merit of *p*-type $Bi_{1-x}Sb_x$ ($0.12 < x < 0.14$) Alloys at Low Temperatures, *Physics of the Solid State* **24**(6), 1881 – 1884 (1982).
7. S. Golin, Band Model for Bismuth-Antimony Alloys, *Phys. Rev*. **176** (3), 830 (1968).
8. B. Lenoir, M. Cassart, J.-P. Michenaud, H. Scherrer, and S. Scherrer, Transport Properties of *Bi*-rich *Bi-Sb* Alloys, *J.Physics and Chemistry of Solids* **57** (1), 89 – 99 (1998).

9. B. Lenoir, A. Dauscher, M. Cassat, Yu. Ravich, and H. Sherrer, Effect of Antimony Content on the Thermoelectric Figure of Merit of $Bi_{1-x}Sb_x$ Alloys, *J. Phys. Chem. Sol*. 59, 129 (1998).
10. L.D. Hicks, M.S. Dresselhaus, Effect of Quantum-Well Structures on the Thermoelectric Figure of Merit, *Phys. Rev. B* 47, 12727-31 (1993).
11. O. Rabin, Y.-M. Lin, and. M. Dresselhaus, Anomalously High Thermoelectric Figure of Merit in $Bi_{1-x}Sb_x$ Nanowires by Carrier Pocket Alignment, *Appl. Phys. Lett.* **79**(1), 81 – 83 (2001).
12. J. Heremans, C.M. Thrush, Yu-Ming Lin, S. Cronin, Z. Zhang, M.S. Dresselhaus, and J.F. Mansfield, Bismuth Nanowire Arrays: Synthesis and Galvanomagnetic Properties, *Phys. Rev. B* 61, 2921 (2000).
13. Shuang Tang and Mildred S. Dresselhaus, Electronic Phases, Band Gaps, and Band Overlaps of Bismuth Antimony Nanowires, *Phys. Rev. B* 89, 045424 (2014).
14. R. Venkatasubramanian, E. Siivola, T. Colpitts, and B. O'Quinn, Thin-Film Thermoelectric Devices with High Room-Temperature Figures of Merit, *Nature* **413**(6856), 597 – 602 (2001).
15. T.C. Harman, P.J. Taylor, M.P. Walsh, and B.E. LaForge, Quantum Dot Superlattice Thermoelectric Materials and Devices, *Science* **297**(5590), 2229-32 (2002).
16. J.P.Heremans, Low-Dimensional Thermoelectricity, *Acta Physica Polonica A* **108**(4), 609 – 634 (2005).
17. Liang Fu, C.L. Kane, and E.J. Mele, Topological Insulators in Three Dimensions, *Phys. Rev. Let.* 98, 106803 (2007).
18. A.A. Taskin, Kouji Segawa, and Yoichi Ando, Oscillatory Angular Dependence of the Magnetoresistance in a Topological Insulator $Bi_{1-x}Sb_x$, *Phys. Rev. B* 82, 121302(R) (2010).
19. Ryuji Takahashi and Shuichi Murakami, Thermoelectric Transport in Topological Insulators, *Semiconductor Science and Technology* **27**(12), 124500 (2012).
20. Liang Fu, C.L. Kane, Topological Insulators with Inversion Symmetry, *Phys. Rev. B* 76, 045302 (2007).
21. N.B. Brandt, G.I. Golysheva, Nguyen Minh Thu, M.V. Sudakova, and Ya.G. Ponomarev, Origination of Saddle Point in the Energy Spectrum $Bi_{1-x}Sb_x$ Alloys at Inversion of Bands with a Change in Composition *x*, *Low Temperature Physics* **13**(11), 1209 – 1212 (1987).
22. D. Hsieh et al., Observation of Unconventional Quantum Spin Textures in Topological Insulators, *Science* 323(5916), 919 – 922 (2009).
23. Akinori Nishide, Alexey A. Taskin, et al. Direct Mapping of the Spin-Filtered Surface Bands of a Three-Dimensional Quantum Spin Hall Insulator, *Phys. Rev. B* 81, 041309(R) (2010).
24. D. Hsieh, D. Qian, L. Wray, Y. Xia, Y.S. Hor, R.J. Cava, and M.Z. Hasan, A Topological Dirac Insulator in a Quantum Spin Hall Phase, *Nature* **452**(7190), 970 – 974 (2008).
25. Dong-Xia Qu, Sarah K. Roberts, and George F. Chapline, Observation of Huge Surface Hole Mobility in the Topological Insulator $Bi_{0.91}Sb_{0.09}$ (111), *Phys. Rev. Lett*. 111, 176801 (2013).
26. T.H. Wang, H.T. Jeng, Enhanced Thermoelectric Performance in Thin Films of Three-Dimensional Topological Insulators, *arXiv:1608.00348* [cond-mat.mes-hall], 2016.
27. A. Nikolaeva, T.E. Huber, D. Gitsu, and L. Konopko, Diameter Dependent Thermopower of Bismuth Nanowires, *Phys. Rev. B* 77, 035422 (2008).
28. Albina A. Nikolaeva, Leonid A. Konopko, Tito E. Huber, Pavel P.Bodiul, and Ivan A.Popov, Prospects of Nanostructures $Bi_{1-x}Sb_x$ for Thermoelectricity, *J.Solid State Chemistry* 193, 71 – 75 (2012).
29. N.B. Brandt, D.V. Gitsu, A.A. Nikolaeva, and Ya.G. Ponomarev, Investigation of Size Effects in Thin Cylindrical Bismuth Single Crystals in a Magnetic Field, *Sov. Phys. JETP* **45**(6) 1226 (1977).

30. D.V. Gitsu, I.M. Golban, V.G. Kantser, and F.M. Muntiany, *Transport Phenomena in Bismuth and its Alloys* (Kishinev: Stiinţa, 1983), 266 p.
31. A. Nikolaeva, T. Huber, L. Konopko, and A. Tsurkan, Observation of the Semiconductor-Semimetal and Semimetal-Semiconductor Transitions in *Bi* QuantumWires Induced by Anisotropic Deformation and Magnetic Field, *Low Temp Phys* 158, 530 – 535 (2010).
32. D. Gitsu, L. Konopko, A. Nikolaeva, and T. Huber, Pressure Dependent Thermopower of Individual *Bi* Nanowires, *J. Applied Physics Letters* 86, 10210 (2005).
33. T.W. Cornelius, M.E. Toimil-Molares, R. Neumann, G. Fahsold, R. Lovrincic, A. Pucci, and S. Karim, Quantum Size Effects Manifest in Infrared Spectra of Single Bismuth Nanowires, *Appl. Phys. Lett.* 88, 103114 (2006).
34. Jane E. Cornett and Oded Rabin, Thermoelectric Figure of Merit Calculations for Semiconducting Nanowires, *Appl. Phys. Lett*. 98, 182104 (2011).
35. Shuang Tang and Mildred S.Dresselhaus, Constructing Anisotropic Single-Dirac-Cones in $Bi_{1-x}Sb_x$ Thin Films, *Nano Lett.* **12**(4), 2021 – 2026 (2012).

Submitted 10.08.2016